N-Terminal Modification of Gly-His-tagged Proteins with Azidogluconolactone.

‡Karl D. Brune[*,a,b], ‡Ilva Liekniņa[c], ‡Grigorij Sutov[a,d], ‡Alexander R. Morris[a,d,e], Dejana Jovicevic[a], Gints Kalniņš[c], Andris Kazāks[c], Rihards Kluga[f,g], Sabine Kastaljana[f,g], Anna Zajakina[c], Juris Jansons[c], Dace Skrastiņa[c], Karīna Spunde[c], Alexander A. Cohen[h], Pamela J. Bjorkman[h], Howard R. Morris[e,i], Edgars Suna[f,g], Kaspars Tārs[*,c,g]

[a] Genie Biotech Ltd, Beachside Business Centre, Rue du Hocq, St. Clement, JE2 6LF, U.K.
[b] Department of Bioengineering, Imperial College London, SW7 2AZ, U.K.
[c] Latvian Biomedical Research and Study Centre, Ratsupites 1, 1067 Riga, Latvia.
[d] Lab Group LT, UAB, Vilnius, Lithuania.
[e] BioPharmaSpec Ltd, Suite 3.1, Lido Medical Centre, St. Saviour, JE2 7LA, U.K.
[f] Latvian Institute of Organic Synthesis, Aizkraukles 21, 1006 Riga Latvia.
[g] University of Latvia, Jelgavas 1, 1004 Riga, Latvia.
[h] Division of Biology and Biological Engineering, California Institute of Technology, Pasadena, CA 91125, U.S.A.
[i] Department of Life Sciences, Imperial College London, SW7 2AZ, U.K.
[*] K.D.B. - brune.karl@gmail.com; K.T. - kaspars@biomed.lu.lv
‡These authors contributed equally.
Supporting information for this article is given via a link at the end of the document.

Abstract: Site-specific protein modifications are vital for biopharmaceutical drug development. Gluconoylation is a non-enzymatic, post-translational modification of N-terminal HisTags. We report high-yield, site-selective *in vitro* α-aminoacylation of peptides, glycoproteins, antibodies, and Virus-like particles (VLPs) with azidogluconolactone at pH 7.5 in 1 h. Conjugates slowly hydrolyse, but diol-masking with borate esters inhibits reversibility. In an example, we multimerise azidogluconoylated SARS-CoV-2 receptor-binding domain (RBD) onto VLPs via click-chemistry, to give a COVID-19 vaccine. Compared to yeast antigen, HEK-derived RBD was immunologically superior, likely due to observed differences in glycosylation. We show the benefits of ordered over randomly oriented multimeric antigen display, by demonstrating single-shot seroconversion and best virus-neutralizing antibodies. Azidogluconoylation is simple, fast and robust chemistry, and should accelerate research and development.

Introduction

Bioconjugation is crucial for chemical biology and biopharmaceutical development. Traditional methods target naturally-occurring biomolecule functional groups, such as amines (Lys, N-terminus), carboxyls (Asp, Glu, C-terminus), or sulfhydryls (Cys).[1,2] Multiple-activation can cause heterogeneous populations with possibly different biological activities and in some cases undesirable protein-protein cross-linking, complicating analysis.[3]

More than >80% of proteins in the Protein Data Bank (PDB) have exposed N-termini.[4] Importantly, the α-amino group can be selectively targeted because its pK_a is lower (6-8) than that of typical Lys ε-amines (~10.5).[4] Several powerful N-termini-specific chemical and enzymatic strategies have been developed.[1,3–5] However, depending on application some drawbacks include: the need for reducing (Schiff-base) or oxidizing agents [Ser/Thr-targeting[6], *ortho*-(imino)quinones[7]], Nt.-Cys [native chemical ligation, 2-formyl phenylboronic acid[8]], special buffer requirements (solvents, pH, imidazole-1-sulfonyl azide[9]], uncontrollable conjugate reversibility [hydrazones[6], 2-pyridinecarboxaldehyde (2PCA)[10]], high reaction temperature (≥37 ºC), lengthy reaction times (>1h) and low yields (<50%).

His-Tags are metal ion coordinating motifs, widely used for recombinant protein purification via immobilized metal affinity chromatography (IMAC).[11] Historically His-Tags have been met with scrutiny due to possible nickel leaching from affinity resins. However in 2014, the FDA first approved a His-tagged biotherapeutic[12] and this regulatory paradigm shift may pave the way for future His-Tagged biologicals - as of 2021 His-tagged oportuzumab monatox is under review.[13]

Gluconoylation is a non-enzymatic post-translational modification caused by spontaneous reaction of pentose phosphate pathway intermediates with protein amino groups.[14–16] Acylation with glucono-1,5-lactone (GDL) also occurs *in vitro*, and His-flanked α-amines are extraordinarily prone.[14,17–19] Most studies focus on abolishing gluconoylation[20,21], and little use was made of its selectivity. In 2018, the Jensen group reported substituted methoxyphenyl esters as acylating reagents for N-terminal Gly-$His_{(n)}$-tags.[19] Difficult GDL derivative synthesis, and perhaps unexpected gluconoyl reversibility may have motivated the choice for methoxyphenyl esters, whose drawbacks were nevertheless found to be lower yields (~50-80%) and increased off-site (~10-20%) labelling compared to GDL (>90% yield, <2% off-site labelling).[19]

Here we report chromatography-free azido-GDL derivative synthesis for Gly-His acylation. We show high yield and N-terminal selectivity and inhibit gluconoyl reversibility with borate. We react the installed azide via both copper(I)-catalysed, and strain-promoted azide-alkyne cycloaddition (CuAAC/SPAAC). To showcase the usefulness of the reaction, we build a COVID-19 vaccine by multimerizing azidated antigen to a bacteriophage VLP via SPAAC. We demonstrate that mammalian-expressed antigen performs better immunologically than yeast-derived material, which we rationalize is due to the observed differences in glycosylation. The candidate causes single shot seroconversion, and induces virus-neutralizing antibodies (n/Abs).

Results and Discussion

Scope and robustness of gluconoylation

We GDL-acylated several His-Tagged model proteins, all showing high mono- and minimal dual labelling. Proteins without Gly-His-Tag, or with C-terminal HisTag and proximal Lys (-H_6-SSK) did not react efficiently (Table S1). Conversely, 2PCA-labelling of poorly or non-reactive GDL substrates showed conversion (see e.g. Figure S8), proving α-amino-group availability. Whereas 2PCA labels N-termini indiscriminately[10], GDL shows preference for *specific* Gly-terminated N-termini. As expected, pre-reacting substrates with 2PCA prohibited subsequent labelling with GDL (Figure S9). Given reports of *in vivo* gluconoylation *without* N-terminal HisTags, we tested a

small peptide library and observed that GGKWSKR[22], GASGSKG[23] and GG also react well (Table S2). Thus proximal His-residues are beneficial for the reaction, but are not an absolute requirement.

Reacting GDL with the popular GSS-H_6-Tag for 1 h, we find that varying label concentration (25-200 mM) greatly influenced yield but protein molarity did not (10-140 µM) (Figure S18A,B). Labelling with low GDL (25 mM) for longer (>1.5 h) gave better yields at 4 ºC (80-90%), but not at 22 ºC (~65%) (Figure S19). Similarly, reacting with 50 mM GDL for 1 h at 4 or 22 ºC gave higher conversion versus 37 ºC. (Figure S18C). We reason that GDL hydrolysis is reduced at lower temperatures[24], but substrate reactivity is reduced less so. 1 M NaCl and 5 M guanidinium chloride reduced yield, but glycerol, detergents or 5 M urea did not (Figure S18D).

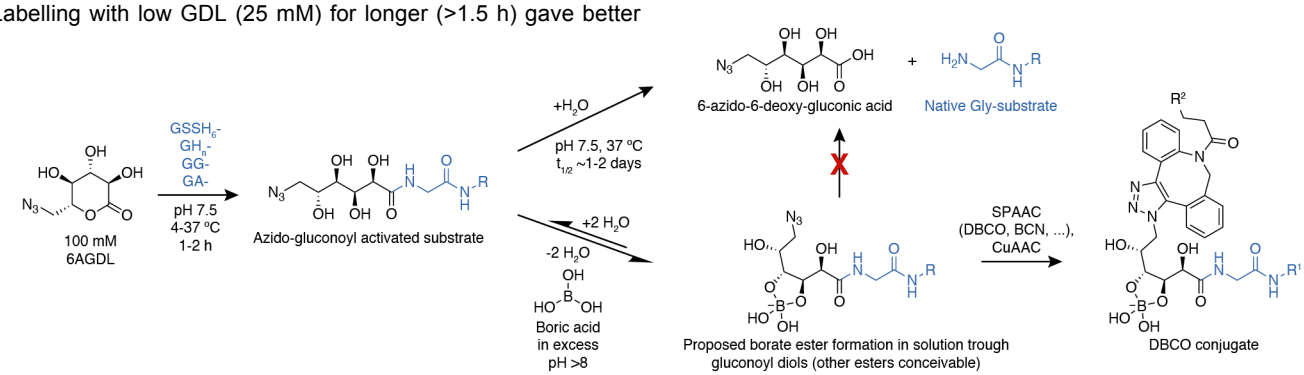

Scheme 1. **Azidogluconoylation and reversibility modulation.** Gly-His_n tagged peptides and proteins are selectively labelled at their N-termini with 6-azido-6-deoxy-D-glucono-1,5-lactone (6AGDL). Borate-diol ester formation inhibits conjugate hydrolysis. In a secondary step, the installed azide group is reacted with click-chemistry reagents (SPAAC, CuAAC, etc.).

Azidogluconoylation

We envisioned GDL derivatives with an azido-handle (Scheme 1). Because of 6-azido-6-deoxy-glucose being most SPAAC-reactive[25], and reports of *in vivo* 6-phosphogluconoylation[14], we presumed that 6-substitution may maximize click chemistry accessibility, whilst least affecting lactone reactivity. We used Shvo's catalyst for oxidation.[26] With the lactone in hand, we tested labelling of an His-tagged Affibody (GSS-H_6-AffiEGFR).[27] Deconvolution of multiply charged experimental species gave the expected masses, with near complete conversion and minimal bi-labelling (~1%, LC-MS) (Figure 1, Figure S20). MS sequencing of tryptic digests confirmed the N-terminus as the main target (Figure S21A-C). We also observed an unreactive species due to host-derived N^{α}-acetylation, thus no 6AGDL-labelling occurred (Figure 1, Figure S21D). Host-acetylation was later reduced with $MgSO_4$.[28] Slightly increasing dual-functionalization could be observed with increasing pH (0.3% at pH 7.0, 0.8% at pH 7.5, ~4.4% at pH 8.2), and yields were generally lower at lower pH (12% at pH 5, 40% at pH 7, 85% at pH 7.5, and 84% at pH 8.2; using 100 mM 6AGDL, 1 h, room temperature) (Figure S23).

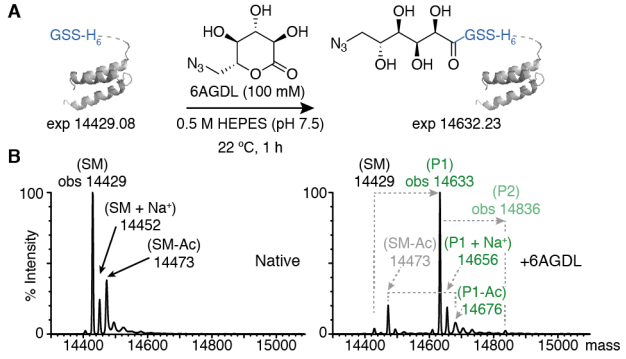

Figure 1. **Functionalization of GSS-H_6-AffiEGFR. (A)** Reaction scheme. Not to scale. **(B)** Deconvoluted spectra of native (left), and modified (right) protein (Q-TOF). SM: starting material; SM-Ac: acetylated SM; P1: singly-labelled product; P2: doubly-labelled product. MALDI-TOF MS showing near-complete conversion (Figure S22).

Antibody drug conjugates (ADCs) are potent therapeutics. mAb N-termini are rarely modified, as proximity to complementarity-determining regions (CDR) may affect binding.[29] However, N-terminal mAb labelling does not necessarily affect binding. For example, modification of an anti-EphA2 mAb on its light chain (~1 kDa payload)[30], or modification of trastazumab on CDR-proximal heavy and light chain N-termini (~850 Da payload) had little to no effect on binding affinity and kinetics.[31] Monoclonal antibodies (mAbs) with CDR-distal N-termini, e.g. durvalumab and atezolizumab, may be even more tolerable (Figure S24).[32] We GH_6-tagged atezolizumab's heavy chain, to specifically target the distant termini. N-terminal sequence modification of proteins expressed via mammalian secretion can sometimes yield N-terminally inhomogeneous preparations due to incorrect signal peptide cleavage.[29] Expression of the GH_6-tagged mAb gave the expected masses however, and only mAb-common C-terminal Lys deficiency was observed.[33] 6AGDL-labelling gave predominantly di-modified mAb, with high selectivity for the tagged heavy chain over the light chain observed by MS after reduction. Some heavy chain ε-amine activation was observed (~2.5%), which may be expected for a molecule with 31 Lys (Figure 2).

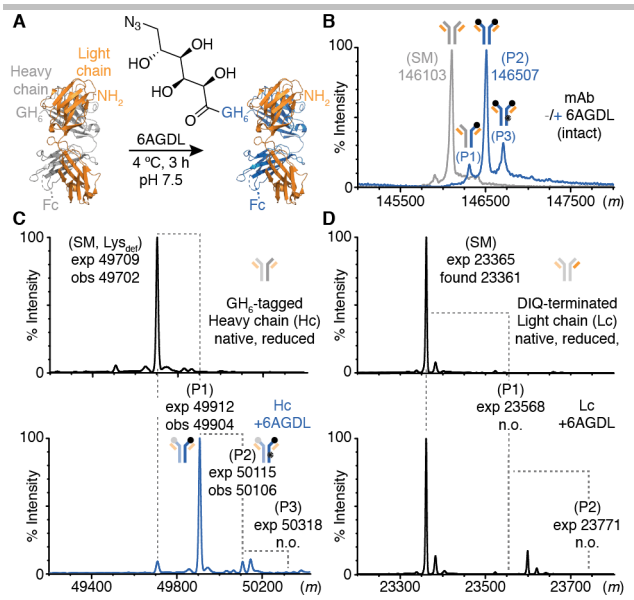

Figure 2. **Heavy-chain specific N-terminal mAb labelling with 6AGDL. (A)** mAb reaction scheme (PDB 5XXY). 40 µM mAb, 0.25 M HEPES pH 7.5, 100 mM 6AGDL, 4 °C for 3 h. **(B)** Intact MS overlay. Atezolizumab with GH_6-heavy chain before (grey) and after (blue) labelling. MS of the **(C)** heavy, and **(D)** light chain, showing azidogluconoylation of the heavy but not the light chain (DTT-reduced). *m*: mass; n.o. – not observed. Not to scale.

Phage-derived coat proteins can self-assemble into MDa-sized VLPs and are being developed as vaccine and therapeutic carriers.

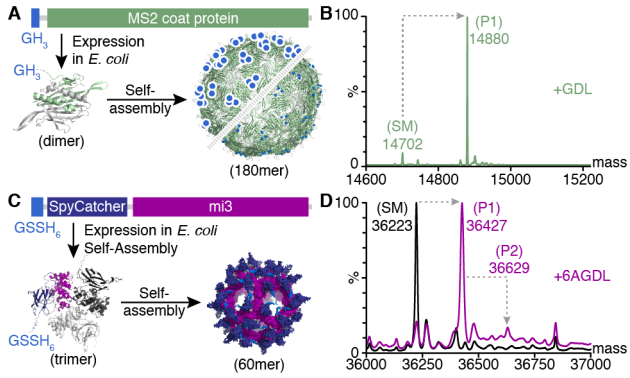

Figure 3. **(6A)GDL modification of megadalton protein nanoparticles. (A,C)** Scheme for biosynthesis of nanoparticles (PDB 2MS2, SpyCatcher-mi3 trimer was modelled with AlphaFold v2.0[34] and PDB 7B3Y was used for alignment). Blue circles indicate approximate N-termini positions. Not to scale. **(B,D)** MS of modified GH_3-MS2 (~140 µM, reduced), and $GSSH_6$-SpyCatcher003-mi3 (~140 µM, overlay) after 1 h with 100 mM (6A)GDL at pH 7.5, 22 °C. See Figure S25 for further nanoparticles, and (6A)GDL labelling.

N-terminal GH_3-tagging the coat proteins of the bacteriophages MS2[35], PQ-465[36], Shahe1[37], and AP205d (single-chain dimer)[38] permitted VLP assembly, IMAC purification, and (6A)GDL labelling. $GSSH_6$-tagged "Plug-and-Display" SpyCatcher-mi3[39,40] protein nanoparticles also reacted (Figure 3, Figure S25). However, not all VLP-fusions were Gly-His compatible in our hands. We failed to obtain assembled GH_3-tagged Qβ, likely due to quasi-3-fold axis crowding[41]; whereas GH_3-2PP7[42] likely assembled (as indicated by NAGE), but quickly aggregated (visual observation, data not shown).

Table 1. **Acylation with 100 mM 6AGDL.** Proteins were reacted for 1 h, pH 7.5 (unless stated otherwise). Protein concentrations varied (10-100 µM). Yields are estimated by MS (%, n=1). See Supporting Information for details.

Protein	N-term.	P1	P2	kDa	Lys	Figure
SUMO	$GSSH_6$	96	9	12	9	Figure S27B
SUMO (pH 7.4)	$GSSH_6$	90	3.9	12	9	Figure S27C
Cys-SpyCatcher[a]	GH_6DC	86	0.3	12	8	Figure S28
SUMO-H_6-SSK	GSS	17	0.3	13	10	Figure S29
SUMO-SpyTag	$GSSH_6$	95	1.7	14	11	Figure S30
SnoopCatcher	$GSSH_6$	97	0.9	14	9	Figure S31
AffiEGFR	$GSSH_6$	97	1.3	14	10	Figure 1
ZZ	$GSSH_6$	93	0.1	15	12	Figure S32
hRBD	GH_6	[c]>90	~2	22	8	Figure S33
Cys-SpyCatcher[b]	GH_6DC	86	≤2	24	16	Figure S34
Flagellin	GH_6	83	2.7	32	15	Figure S35
Protein A	$GSSH_6$	95	n.o.	36	26	Figure S36
SpyTag-MBP	$GSSH_6$	94	3.8	44	38	Figure S37
Atezolizumab (Hc)	GH_6	[d]85	2.5	49	31	Figure 2
MS2	GH_3	[e]93	0.1	14	6	Figure S25
SpyCatcher-mi3	$GSSH_6$	85	n.d.	36	28	Figure S25

[a] Monomer, [b] dimer, [c] 90 min at 4 °C, [d] 3 h at 4 °C, [e] reported as the gluconoyl yield. n.o. – not observed; n.d.- not determined.

We summarize results in Table 1. We observed SUMO dual-activation, which could be reduced from ~10% (pH 7.5) to <4% (pH 7.4). Catcher/Tag[27,43] proteins also showed high yield upon 6AGDL labelling. Both gluconoylated SpyCatcher and SpyTag have been previously reported to react with their respective cognate partner.[43,44] N-terminally azidated SpyTag has also been reported to react with SpyCatcher.[45] We find Catcher/Tag reactivity is also retained after azidogluconoylation of either Catcher or Tag - or both. Moreover, the Catcher/Tag reaction also proceeded in parallel to azidogluconoylation (Figure S38). Remarkably, we observed high yield 6AGDL-conversion for GG-peptides after labelling twice at 4 °C (>95%, Figure S39, Figure S40). Next, we reacted azidated substrates via CuAAC[46] and SPAAC. Propargylamine, DBCO[47] (Figure S45), alkyne-PEG (Figure S46), and BCN[48] (Figure S47); all gave the expected products in good yield.

At is "optimal" concentration, 6AGDL - like GDL[19] - is faster (1 vs. 24 h), higher yielding (>95 vs. ~50%), and more selective (<1 vs. 5% offsite) than 4-methoxyphenyl 2-azidoacetate at its respective "optimal" concentration[19] (Table S3, Figure S42). We provide evidence that 4-methoxyphenyl 2-azidoacetate at 100 mM may also label residues other than α- and or ε-amines (Figure S43).

Reversibility and polyol manipulation

Similar to recent reports[19,49] we observe gluconoyl hydrolysis, its rate being dependent on substrate, N-terminal sequence (Table S4), pH (Figure S48) and temperature (Figure S49, Figure S50). For long-term storage, hydrolysis could be limited by freezing or lyophilisation (Figure S50). Simple aldonamides have been proposed to hydrolyse through neighbouring aliphatic hydroxyl group(s)[50], and 4-hydroxylbutyramide hydrolyses via its ɣ-hydroxyl.[51] 6AGDL-modified material reversed slightly slower than GDL-modified protein (Figure S51). To probe the other label hydroxyls, we synthesized 3- and 4-azido-*n*-deoxy-gluconoyl derivatives, which however still reversed (not shown).

Gluconamide hydroxyls react with boron compounds[18,52], mostly via diol borate ester formation.[53] Inspired by (pro)-drug diol masking[54], we added boric acid to the gluconoyl-conjugate solution, which dose-dependently slowed (>5 mM) reversibility in slightly alkaline pH. Higher borate concentrations were required at pH 6.0 (>50 mM), and no inhibition was observed at pH 4, pointing to the pK_a of boric acid as limiting (Figure S52).

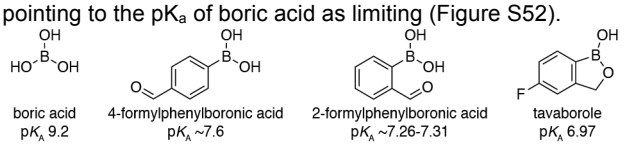

Figure 4. **Exemplary boric acid derivative library members.** For a full list see Figure S53. p*K*a values from literature.[55]

Phenylboronic acid derivatives with lower pK_as are known. After testing a small library (n=7, Figure 4), we identified compounds, which inhibited reversibility at pH 7.5, 50 ºC, overnight - where boric acid failed (Figure S53). Whereas tavaborole showed good overnight inhibition at 50 ºC (Figure S53), it did not provide protection over 5 days (Figure S54). 5 mM 2-formylphenylboronic acid provided the best inhibition over 5 days (Figure S54). Its diol-esters were unobservable by MALDI TOF-MS, but could be reacted with hydroxylamine[56] to form observable covalent adducts, resistant to 0.1% (v/v) trifluoroacetic acid during C18 desalting. For a gluconoyl-peptide we observed two signals, but only one for an azidogluconoyl-peptide (Figure S55, Figure S56).

The C4, and/or C5 hydroxyl likely attack intermolecularly, causing conversion from modified to native protein. We propose that boric acid masks reactive hydroxyls, and/or induces unfavourable steric strain, inhibiting reversibility (Scheme 1). For 2-formylphenylboronic acid, gluconoylated substrate gives two esters, one of which may be the 5,6-, whereas 6-azido-6-deoxy-gluconoylated material only yields one (Scheme S4, Scheme S5). Further studies will be required to elucidate which exact (transient) species form upon boric and 2-formylphenylboronic acid treatment. A recent NMR gluconamide study with phenylboronic acid and benzoboroxole suggests bi- and tridentate complexes.[52]

Borate is present in human tissues[57] and is used as an “inactive ingredient” in FDA-approved IV drugs.[58] Importantly, azidogluconoylated substrates also click-react in borate buffer (Figure S45). Hence practical conjugate storage appears feasible. Based on our *in vitro* pH data, we presume that upon administration borate-diol esters would hydrolyse, initiating reversibility due to change in pH and dilution of boric acid – however kinetics may be affected by natively present polyols, necessitating further studies. We later show that the conjugate bond is sufficiently long lasting *in vivo* to induce a meaningful biological effect (immunization studies) – stable *in vivo* at least on the timescale of a few hours, as required for lymph node drainage.[59] It is conceivable that the 2-formylphenylboronic acid/hydroxylamine reacted gluconoyl bond would be stable indefinitely *in vivo*, but further studies are required.

Practical label-polyol use is also made with methacrylamido phenylboronate SDS-PAGE (mP-AGE).[18] The small azidogluconoyl label (203 Da) resolves from large (>30 kDa) proteins, such as Flagellin and MBP, enabling label monitoring without MS (Figure S57A,B). For many bioconjugation strategies, the purification of modified from unmodified protein can be challenging. The label-polyol interaction with boronic acids can also be leveraged here in non-denaturing boronic acid affinity chromatography (BAC)[60], either in isocratic or trapping mode (Figure S57D,E).

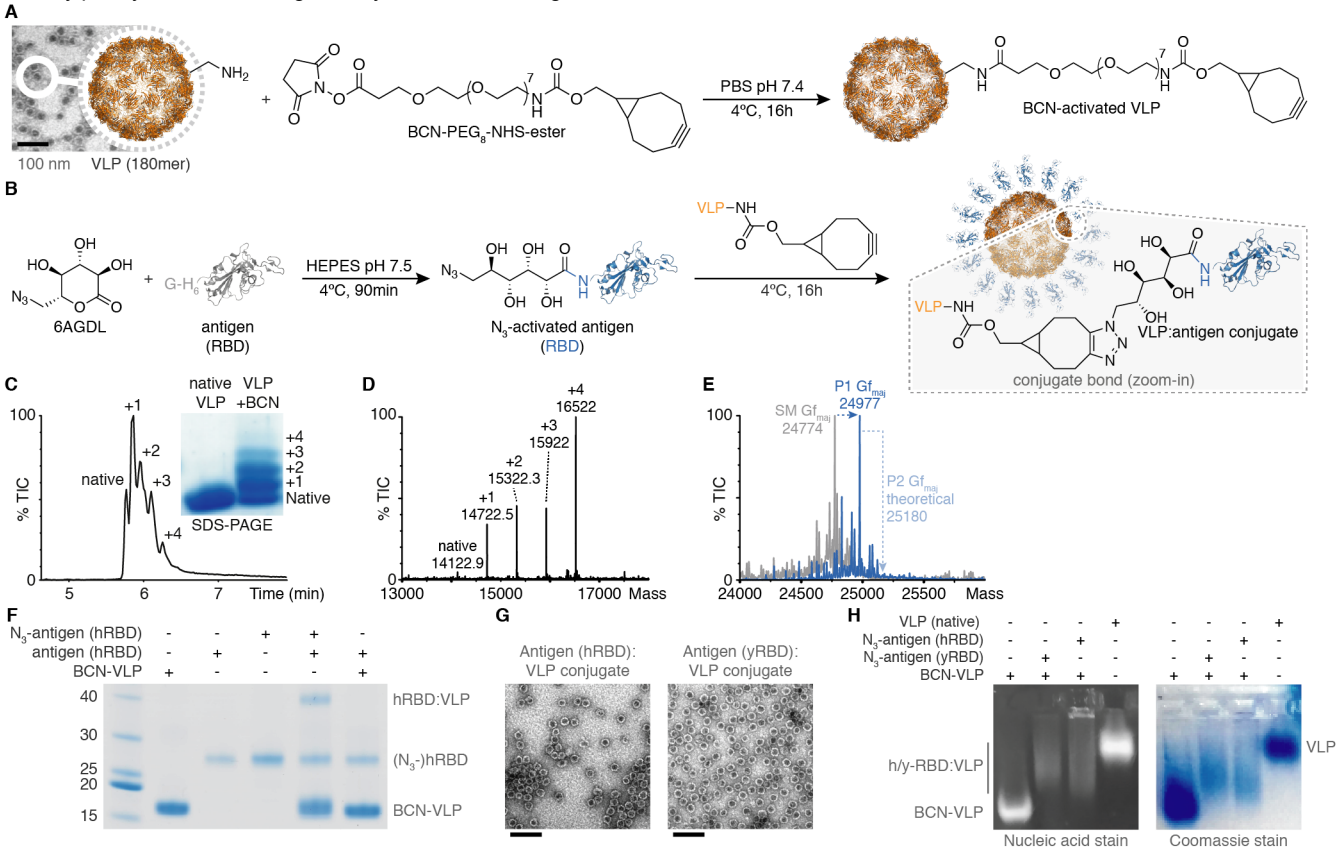

Figure 5 **VLP:antigen conjugate assembly and characterization. (A)** BCN-activation of VLPs. **(B)** Azidogluconoylation of antigen (RBD), and subsequent coupling to activated VLPs. Not to scale. **(C)** LC/MS (C18) separation of native and (multiply) activated VLP monomer. Inset shows reducing SDS-PAGE of native and activated VLP. **(D)** MS of activated VLP monomer (+4 peak). **(E)** MS of 6AGDL-activated hRBD **(F)** Activated VLPs were incubated with activated N_3-antigen

(hRBD) or negative control (115 μM VLPs, 50 μM RBD), before analysis by reducing SDS-PAGE. **(G)** Negatively-stained transmission electron microscopy (TEM) of h/yRBD-conjugated VLPs. Scale bar 100 nm. **(H)** Native agarose gel electrophoresis. See Figure S58 *ff.* for details.

Rapid generation of vaccine candidates

In 2020, COVID-19 became pandemic and the SARS-CoV-2 receptor-binding domain (RBD) emerged as a prime vaccine target. Monomeric antigen can be poorly immunogenic, and its multimerisation can confer single shot seroconversion and better Ab responses.[61] To multimerise the RBD, we chose bacteriophage-derived Qβ VLPs[62] due to their dramatic scalability (>10 g/L in *E. coli*)[63], immune-stimulating RNA[64], and clinical safety.[65] Qβ VLPs consist of 180 coat protein copies assembled into an icosahedral capsid (~28 nm, PDB 1QBE).[41] We reacted yeast and HEK-expressed Gly-His-RBD (y/hRBD) with 6AGDL; and VLP amines with BCN-PEG_8-NHS ester (Figure 5A,B). VLP coat protein was efficiently activated, showing multiple (up to 4) BCN additions, both by LC/MS and reducing SDS-PAGE. However, some native material did not react (native: ~28%, singly-activated: ~37%, doubly-activated: ~24%, triply-activated: ~9%, quadruply-activated: ~2%; Figure 5C,D). hRBD mono-activation across glycoforms was observed by LC/MS and was estimated to be ~90% (Figure 5E, Figure S33).

We removed excess reagents by dialysis or filtration, and incubated activated RBD and VLPs together overnight. Reducing SDS-PAGE and in-gel digestion of the conjugate band (Figure 5F) showed both VLP and RBD peptides. Based on densitometry and the assumption that RBD, coat protein and conjugate stain similarly on a molar basis, we estimate ~30% coupling efficacy for the activated RBD. Using the same assumption, we estimate that RBD coupling to the VLP was ~10-15%, equating to 18-27 RBDs per VLP. It is known that high conjugation yields can translate to higher antibody titres for small Mw haptens, and high (>90%) antigen density is commonly assumed to be also beneficial for protein antigen VLP conjugates. However, high conjugation yield is no absolute requirement for generation of potently immunogenic protein VLP-conjugates. Two doses of a malarial antigen coupled HBsAg at only 10% gives significant responses[66], and as little as 5 antigen copies can be sufficient for maximal B-cell activation.[67] Higher VLP:RBD conjugation yields may be achieved by increasing molarities of both partners.

Size-exclusion chromatography into the void, followed by TEM and NAGE showed nucleic acid packaging particles consistent with VLPs (Figure 5G,H). We monitored activated RBD over 4 months, finding minimal reversibility (borate buffer, stored at 4ºC, Figure S63).

Neutralizing Abs also target viral glycans.[68] When comparing glycoproteomic N343(hRBD) data to previous work[69,70], we observe complex N-glycans bearing LacdiNAc antennae with and without fucosylation (Figure S64, Figure S65).[70] To the best of our knowledge, we present for the first time a detailed comparative glycan characterization of yeast-derived RBD, demonstrating families of high mannose N-glycans, with and without phosphorylation (Figure S66, Figure S67, Figure S68), and these two glycoprotein antigens were then compared in the immunization studies below.

Oriented antigen display may produce better quantitative and qualitative Abs than random display.[71] To test this, we randomly activated RBD with NHS-tetrazine ester **6**, observing multiple activation even with careful titration (Figure S69). Activated tetrazine-RBDs were coupled to BCN-NHS-ester(**15**)-activated VLPs via Inverse-Electron-Demand Diels−Alder[72] (Scheme S3). Observed precipitation was likely due to multiply-activated RBD cross-linking VLPs (Figure S61, Figure S70). After trial and error, we generated sufficient soluble particulate material for immunizations (TEM Figure S60).

Immunizations

We primed mice with y- and hRBD conjugates, native, and activated monomer, all adjuvanted with AddaVax. Immunizations were well tolerated and no obvious side effects were observed. Anti-RBD ELISA on day 14 showed single shot seroconversion for all hRBD:VLP (6AGDL) conjugate group animals (Figure S71A). Conversely, booster shots were required for seroconversion with monomer RBD formulations, and randomly decorated (NHS) VLPs (Figure S71B). Titres increased in all groups after boosting on day 28 and 42 (Figure S71B,C). 6AGDL-activated monomeric hRBD gave higher titres than native proteins, which may be due to activation or aggregation (Figure S71C). Moderate Ab responses against the HisTag were detected using a non-related His-tagged bait after immunizing with adjuvanted activated protein (Figure S71D). Titres against the VLP were lower for the conjugate groups compared to just VLP immunization, possibly due to carrier shielding by the displayed RBD (Figure S72).

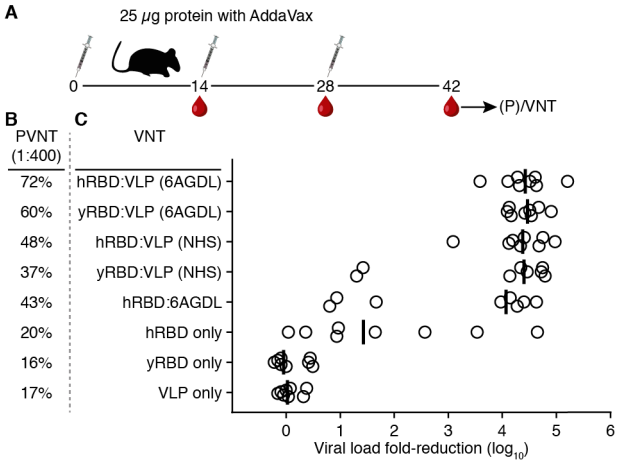

Figure 6. **Neutralizing capacity of sera from vaccinated animals. (A)** Immunization and bleeding schedule of animals (n=8/group). **(B)** Neutralization capacity at 1:400 dilution for each pooled sera group in the PVNT assay. **(C)** Viral load fold-reduction as measured by relative quantitation of RNA of viral against a positive control ($2^{-\Delta\Delta Ct}$). Each circle represents data obtained for individual animal sera tested in triplicate. A vertical line indicates the geometric mean for each group. Statistical analyses are reported in the main text.

To assay the Ab responses in more detail, we evaluated the neutralizing activity elicited by each immunogen in both pseudo- (PVNT), and live virus neutralization (VNT) tests. In VNT, All VLP-multimerised RBD formulations significantly reduced SARS-CoV-2 viral load versus the control group (VLP only) [Kruskal–Wallis test followed by Dunn's multiple comparison test (KW p≤0.001)]. Even though neutralizing activity was observed for some individual animals, monomeric groups did not reach significance (KW p>0.06). When comparing only the monomeric groups, hRBD performed better than yRBD in VNT – which may be due to differences in glycosylation (KW p=0.04, Mann-Whitney p=0.005). No statistical significance was observed for comparing native and activated hRBD (KW p=0.87; Mann-Whitney p=0.23). Of note, inexpensive yRBD, eliciting no neutralization as a monomer, induced strong neutralizing antibodies upon multimerisation and was indistinguishable from

multimeric formulation hRBD at the sera concentration tested (i.e. not significant) (Figure 6). In fact, no statistical difference could be discerned between different conjugation strategies, or multimerised antigen variants at the tested sera dilution, likely due to VNT assay saturation. We tested neutralization activity against pseudotyped virus at different sera dilutions (pooled) to elucidate differences (PVNT). 6AGDL-assembled hRBD:VLP conjugate induced the highest neutralization activity across all dilutions tested followed by yRBD also using 6AGDL. The same antigen trend was found for VLPs assembled via NHS-chemistry, which scored lower than any 6AGDL-conjugate, but higher than native monomeric RBD formulations (Figure S73, Table S10). Individual sera of the three most neutralizing groups were assayed in PVNT. While variability was observed, the average infection inhibition was similar to that of pooled sera, with the hRBD:VLP (6AGDL) group again showing highest neutralizing activities (Figure S74).

The benefits of antigen multimerisation are well established[61], and multimerisation was also favourable here. Using a single VLP, the same antigens, but different chemical conjugation strategies, our data corroborate that *oriented* antigen display in particular can be superior to randomly oriented antigen.[71] Therapeutic Qβ VLPs with CpGs (TLR9) are in clinical phase, and CpGs can increase Ab titres by 5-500 fold[73] Besides the licensed mRNA- and vectored vaccines against COVID-19, reports of promising multimeric RBD protein candidates have been published (Table S13). In April 2021, the furthest clinically-progressed RBD candidate is a Plug-and-Display (Catcher/Tag) RBD on hepatitis B surface antigen (phase II).[66] It is yet unknown if pre-existing Abs in the human population against SpyCatcher and/or HBsAg could be problematic, and whether this could be overcome by increasing dose.[39] The emerging threat of vaccine escape mutants may require additional approaches.[40,74] Possible synergy, also for other antigens, may be obtained by heterologous boosting to circumvent any carrier-induced suppression. To this end, 6AGDL is orthogonal to Catcher/Tag, opening the possibility to conjugate a single antigen to different nanoparticle platforms.

Conclusion

We present azidogluconoylation for site-specific activation of proteins bearing N-terminal Gly-His-tags. High yield labelling occurs in fully aqueous conditions at near neutral pH and various temperatures. Predominant mono-activation is demonstrated for various substrates, including small peptides, glycoproteins, mAbs, and VLPs. The azido-linker is amenable to gram-scale synthesis from inexpensive glucose.

The choice of an “optimal” N-terminal sequence depends on considerations other than chemical reactivity alone, because - as we show - high azidogluconoylation yields can be achieved for most Gly-terminated N-termini by repeated labelling, and modulating reagent concentration, temperature and/or time. N-terminal sequence considerations may include convenience of using pre-existing constructs and commercially available proteins (pET vectors use a $GSSH_6$-tag; with >200,000 constructs cloned), effects of any N-terminal codon changes on translation initiation rate in bacterial expression systems (optimized pET vector with $GSSH_6$-tag preferred for high protein yield[75]), HisTag binding in denaturing conditions (H_6 preferred), His-repeat reduction motivated by minimizing tags to address any regulatory concerns and/or certain *in vivo* applications (GH_{1-3}, or GG/GA), but also the rate of label reversibility (GH_6 reverses faster than $GSSH_6$- or GG-). Preclinically, our group currently prefers G(SS)-H_{3-6} for tagging recombinant proteins, and labelling with 100 mM 6AGDL at pH 7.5 (either in 200 mM HEPES, or straight in imidazole IMAC eluates), either at RT for 1 h, or 2-3 h at 4 ºC for more delicate proteins.

An interesting linker feature is its controllable reversibility, proceeding over days at physiological-like conditions *in vitro*, and yielding native protein. We suggest reversibility to occur through label polyol(s). Boric acid inhibits reversibility *in vitro* via formation of borate-label-diol esters. The borate-diol interaction can also be leveraged to monitor protein activation via mP-AGE, and for protein purification via BAC.

Using the chemistry described here, we rapidly assembled a COVID-19 vaccine candidate by covalently multimerizing the SARS-CoV-2 RBD onto VLPs. hRBD VLPs assembled via 6AGDL induced single shot sero-conversion, and best virus-neutralizing activity. We demonstrate that ordered antigen orientation can be superior to random display. The strategy may be used to display also other (self)-antigens on proteins or synthetic liposomal/polymeric nanoparticles. Importantly, because azidogluconoylation is specific for *specific* N-termini, our strategy reduces the likelihood of ligating mammalian cell derived host cell proteins (HCPs) to VLPs. This is a major concern for Cys-based VLP-conjugation approaches, where conjugation of free Cys-containing HCPs to the VLP could break B-cell self-tolerance upon immunization. Future iterations of this vaccine candidate generation may entail site-specifically activating the Qβ VLP[76], in order to query if any further benefits may be obtained over random VLP-activation as described here.

As with other techniques, azidogluconoylation has advantages and drawbacks compared to other N-terminal labelling strategies (Table S14). The choice for a specific N-terminal targeting strategy will highly application-dependent, and we refer the reader to recent reviews on N-terminal reactions for details.[77,78] The reaction may find use in affinity molecule decoration, to give for example ADCs. It will be of special interest to investigate combinations of azidogluconoylation with other conjugation strategies, apparently unaffected by gluconoylation[43,79], but also to install more reactive handles onto the GDL-scaffold. It will be particularly interesting to explore applications where the optional label reversibility could be beneficial.

Acknowledgements

This research was funded by the Latvian Council of Science (VPP-COVID-2020/1-0014), The Lithuanian Agency for Science, Innovation and Technology (MITA, 01.2.1-MITA-T-852-01-0109), the Merkin Institute for Translational Medicine at The California Institute of Technology, BioPharmaSpec Ltd and Genie Biotech Ltd.

Notes: A.R.M, G.S., and K.D.B are named inventors on Genie Biotech patent applications for azidogluconoylation. All other authors declare no conflict of interest.

Keywords: click chemistry • immunology • nanoparticles • protein modifications • site-specific conjugation.

References

[1] G. T. Hermanson, *Bioconjugate Techniques*, Elsevier, London **2013**.

[2] J. N. deGruyter, L. R. Malins, P. S. Baran, *Biochemistry* **2017**, *56*, 3863–3873.

[3] K. F. Geoghegan, in *Curr. Protoc. Protein Sci.* (Eds.: J.E. Coligan, B.M. Dunn, D.W. Speicher, P.T. Wingfield), John Wiley & Sons, Inc., Hoboken, NJ, USA, **2016**, pp. 15.2.1-15.2.20.

[4] C. B. Rosen, M. B. Francis, *Nat. Chem. Biol.* **2017**, *13*, 697–705.

[5] E. A. Hoyt, P. M. S. D. Cal, B. L. Oliveira, G. J. L. Bernardes, *Nat. Rev. Chem.* **2019**, *3*, 147–171.

[6] K. F. Geoghegan, J. G. Stroh, *Bioconjugate Chem.* **1992**, *3*, 138–146.

[7] A. C. Obermeyer, J. B. Jarman, M. B. Francis, *J. Am. Chem. Soc.* **2014**, *136*, 9572–9579.

[8] H. Faustino, M. J. S. A. Silva, L. F. Veiros, G. J. L. Bernardes, P. M. P. Gois, *Chem. Sci.* **2016**, *7*, 5052–5058.

[9] L. Schoonen, S. Eising, M. B. van Eldijk, J. Bresseleers, M. van der Pijl, R. J. M. Nolte, K. M. Bonger, J. C. M. van Hest, *Bioconjugate Chem.* **2018**, *29*, 1186–1193.

[10] J. I. MacDonald, H. K. Munch, T. Moore, M. B. Francis, *Nat. Chem. Biol.* **2015**, *11*, 326–331.

[11] E. Hochuli, W. Bannwarth, H. Döbeli, R. Gentz, D. Stüber, *Nat. Biotechnol.* **1988**, *6*, 1321–1325.

[12] S. S. Usmani, G. Bedi, J. S. Samuel, S. Singh, S. Kalra, P. Kumar, A. A. Ahuja, M. Sharma, A. Gautam, G. P. S. Raghava, *PLoS One* **2017**, *12*, e0181748.

[13] D. S. Wishart, Y. D. Feunang, A. C. Guo, E. J. Lo, A. Marcu, J. R. Grant, T. Sajed, D. Johnson, C. Li, Z. Sayeeda, N. Assempour, I. Iynkkaran, Y. Liu, A. Maciejewski, N. Gale, A. Wilson, L. Chin, R. Cummings, D. Le, A. Pon, C. Knox, M. Wilson, *Nucleic Acids Res.* **2018**, *46*, D1074–D1082.

[14] K. F. Geoghegan, H. B. Dixon, P. J. Rosner, L. R. Hoth, A. J. Lanzetti, K. A. Borzilleri, E. S. Marr, L. H. Pezzullo, L. B. Martin, P. K. LeMotte, A. S. McColl, A. V. Kamath, J. G. Stroh, *Anal. Biochem.* **1999**, *267*, 169–184.

[15] Z. Yan, G. W. Caldwell, P. A. McDonell, W. J. Jones, A. August, J. A. Masucci, *Biochem. Biophys. Res. Commun.* **1999**, *259*, 271–282.

[16] Z. Yan, G. W. Caldwell, P. A. McDonell, *Biochem. Biophys. Res. Commun.* **1999**, *262*, 793–800.

[17] G. K. Smith, D. G. Barrett, K. Blackburn, M. Cory, W. S. Dallas, R. Davis, D. Hassler, R. McConnell, M. Moyer, K. Weaver, *Arch. Biochem. Biophys.* **2002**, *399*, 195–205.

[18] M. P. Pereira Morais, J. D. Mackay, S. K. Bhamra, J. G. Buchanan, T. D. James, J. S. Fossey, J. M. H. van den Elsen, *Proteomics* **2010**, *10*, 48–58.

[19] M. C. Martos-Maldonado, C. T. Hjuler, K. K. Sørensen, M. B. Thygesen, J. E. Rasmussen, K. Villadsen, S. R. Midtgaard, S. Kol, S. Schoffelen, K. J. Jensen, *Nat. Commun.* **2018**, *9*, DOI 10.1038/s41467-018-05695-3.

[20] J. C. Aon, R. J. Caimi, A. H. Taylor, Q. Lu, F. Oluboyede, J. Dally, M. D. Kessler, J. J. Kerrigan, T. S. Lewis, L. A. Wysocki, P. S. Patel, *Appl. Environ. Microbiol.* **2008**, *74*, 950–958.

[21] C. Schoene, S. P. Bennett, M. Howarth, *Meth. Enzymol.* **2016**, *580*, 149–167.

[22] C. R. Morgan, B. V. Miglionico, J. R. Engen, *Biochemistry* **2011**, *50*, 3394–3403.

[23] A. B. Biter, S. Weltje, E. M. Hudspeth, C. A. Seid, C. P. McAtee, W.-H. Chen, J. B. Pollet, U. Strych, P. J. Hotez, M. E. Bottazzi, *J. Pharm. Sci.* **2018**, *107*, 1468–1473.

[24] E. Miclet, V. Stoven, P. A. M. Michels, F. R. Opperdoes, J.-Y. Lallemand, F. Duffieux, *J. Biol. Chem.* **2001**, *276*, 34840–34846.

[25] J. A. Stewart, C. J. Wilson, B. M. Swarts, *J. Carbohydr. Chem.* **2014**, *33*, 408–419.

[26] M. Bierenstiel, M. Schlaf, *Eur. J. Org. Chem.* **2004**, *2004*, 1474–1481.

[27] G. Veggiani, T. Nakamura, M. D. Brenner, R. V. Gayet, J. Yan, C. V. Robinson, M. Howarth, *Proc. Natl. Acad. Sci. U. S. A.* **2016**, *113*, 1202–1207.

[28] D. G. Christensen, J. S. Orr, C. V. Rao, A. J. Wolfe, *Appl. Environ. Microbiol.* **2017**, *83*, e03034-16, e03034-16.

[29] L. S. Witus, C. Netirojjanakul, K. S. Palla, E. M. Muehl, C.-H. Weng, A. T. Iavarone, M. B. Francis, *J. Am. Chem. Soc.* **2013**, *135*, 17223–17229.

[30] P. Thompson, B. Bezabeh, R. Fleming, M. Pruitt, S. Mao, P. Strout, C. Chen, S. Cho, H. Zhong, H. Wu, C. Gao, N. Dimasi, *Bioconjugate Chem.* **2015**, *26*, 2085–2096.

[31] M. J. Ko, D. Song, J. Kim, J. Y. Kim, J. Eom, B. Sung, Y.-G. Son, Y. M. Kim, S. H. Lee, W.-K. You, J. Jung, *mAbs* **2021**, *13*, 1914885.

[32] H. T. Lee, J. Y. Lee, H. Lim, S. H. Lee, Y. J. Moon, H. J. Pyo, S. E. Ryu, W. Shin, Y.-S. Heo, *Sci. Rep.* **2017**, *7*, 5532.

[33] R. J. Harris, *J. Chromatogr. A* **1995**, *705*, 129–134.

[34] J. Jumper, R. Evans, A. Pritzel, T. Green, M. Figurnov, O. Ronneberger, K. Tunyasuvunakool, R. Bates, A. Žídek, A. Potapenko, A. Bridgland, C. Meyer, S. A. A. Kohl, A. J. Ballard, A. Cowie, B. Romera-Paredes, S. Nikolov, R. Jain, J. Adler, T. Back, S. Petersen, D. Reiman, E. Clancy, M. Zielinski, M. Steinegger, M. Pacholska, T. Berghammer, S. Bodenstein, D. Silver, O. Vinyals, A. W. Senior, K. Kavukcuoglu, P. Kohli, D. Hassabis, *Nature* **2021**, DOI 10.1038/s41586-021-03819-2.

[35] D. D. Brauer, E. C. Hartman, D. L. V. Bader, Z. N. Merz, D. Tullman-Ercek, M. B. Francis, *J. Am. Chem. Soc.* **2019**, *141*, 3875–3884.

[36] J. Rūmnieks, I. Liekniņa, G. Kalniņš, M. Šišovs, I. Akopjana, J. Bogans, K. Tārs, *Sci. Adv.* **2020**, *6*, eabc0023.

[37] I. Liekniņa, D. Černova, J. Rūmnieks, K. Tārs, *Vaccine* **2020**, S0264410X20309166.

[38] M. Shishovs, J. Rumnieks, C. Diebolder, K. Jaudzems, L. B. Andreas, J. Stanek, A. Kazaks, S. Kotelovica, I. Akopjana, G. Pintacuda, R. I. Koning, K. Tars, *J. Mol. Biol.* **2016**, *428*, 4267–4279.

[39] R. Rahikainen, P. Rijal, T. K. Tan, H. Wu, A. C. Andersson, J. R. Barrett, T. A. Bowden, S. J. Draper, A. R. Townsend, M. Howarth, *Angew. Chem.* **2021**, *133*, 325–334.

[40] A. A. Cohen, P. N. P. Gnanapragasam, Y. E. Lee, P. R. Hoffman, S. Ou, L. M. Kakutani, J. R. Keeffe, H.-J. Wu, M. Howarth, A. P. West, C. O. Barnes, M. C. Nussenzweig, P. J. Bjorkman, *Science* **2021**, *371*, 735–741.

[41] R. Golmohammadi, K. Fridborg, M. Bundule, K. Valegård, L. Liljas, *Structure* **1996**, *4*, 543–554.

[42] L. Zhao, M. Kopylov, C. S. Potter, B. Carragher, M. G. Finn, *ACS Nano* **2019**, *13*, 4443–4454.

[43] B. Zakeri, J. O. Fierer, E. Celik, E. C. Chittock, U. Schwarz-Linek, V. T. Moy, M. Howarth, *Proc. Natl. Acad. Sci. U. S. A.* **2012**, *109*, E690–E697.

[44] C. Schoene, J. O. Fierer, S. P. Bennett, M. Howarth, *Angew. Chem.* **2014**, *126*, 6215–6218.

[45] I. Duznovic, A. Gräwe, W. Weber, L. K. Müller, M. Ali, W. Ensinger, A. Tietze, V. Stein, *Small* **2021**, 2101066.

[46] S. I. Presolski, V. P. Hong, M. G. Finn, *Curr. Protoc. Chem. Biol.* **2011**, *3*, 153–162.

[47] M. F. Debets, S. S. van Berkel, S. Schoffelen, F. P. J. T. Rutjes, J. C. M. van Hest, F. L. van Delft, *Chem. Commun.* **2010**, *46*, 97–99.

[48] J. Dommerholt, O. van Rooijen, A. Borrmann, C. F. Guerra, F. M. Bickelhaupt, F. L. van Delft, *Nat. Commun.* **2014**, *5*, 5378.

[49] D. Schweida, P. Barraud, C. Regl, F. E. Loughlin, C. G. Huber, C. Cabrele, M. Schubert, *J. Biomol. NMR* **2019**, DOI 10.1007/s10858-019-00228-6.

[50] M. L. Wolfrom, R. B. Bennett, J. D. Crum, *J. Am. Chem. Soc.* **1958**, *80*, 944–946.

[51] T. C. Bruice, F.-Hans. Marquardt, *J. Am. Chem. Soc.* **1962**, *84*, 365–370.

[52] T. Figueiredo, V. Cosenza, Y. Ogawa, I. Jeacomine, A. Vallet, S. Ortega, R. Michel, J. D. M. Olsson, T. Gerfaud, J.-G. Boiteau, J. Jing, C. Harris, R. Auzély-Velty, *Soft Matter* **2020**, *16*, 3628–3641.

[53] J. A. Peters, *Coord. Chem. Rev.* **2014**, *268*, 1–22.

[54] S. Riegelman, E. Z. Fischer, *J. Pharm. Sci.* **1962**, *51*, 206–210.

[55] K. Kowalska, A. Adamczyk-Woźniak, P. Gajowiec, B. Gierczyk, E. Kaczorowska, Ł. Popenda, G. Schroeder, A. Sikorski, A. Sporzyński, *J. Fluorine Chem.* **2016**, *187*, 1–8.

[56] M. K. Meadows, E. K. Roesner, V. M. Lynch, T. D. James, E. V. Anslyn, *Org. Lett.* **2017**, *19*, 3179–3182.

[57] F. J. Murray, *Biol. Trace Elem. Res.* **1998**, *66*, 331–341.

[58] "Inactive Ingredient Search for Approved Drug Products - Search terms 'boric acid' and 'borate,'" can be found under https://www.accessdata.fda.gov/scripts/cder/iig/index.cfm, **2021**.

[59] M. O. Mohsen, L. Zha, G. Cabral-Miranda, M. F. Bachmann, *Semin. Immunol.* **2017**, *34*, 123–132.

[60] M. B. Espina-Benitez, J. Randon, C. Demesmay, V. Dugas, *Sep. Purif. Rev.* **2018**, *47*, 214–228.

[61] M. F. Bachmann, G. T. Jennings, *Nat. Rev. Immunol.* **2010**, *10*, 787–796.

[62] T. M. Kozlovska, I. Cielens, D. Dreilinņa, A. Dislers, V. Baumanis, V. Ose, P. Pumpens, *Gene* **1993**, *137*, 133–137.

[63] M. Emmerling, F. Hennecke, H. Pfründer, M. Rhiel, P. Steiner, EP1885847B1, **2011**.

[64] A. C. Gomes, E. S. Roesti, A. El-Turabi, M. F. Bachmann, *Vaccines* **2019**, *7*, 47.

[65] P. Pumpens, R. Renhofa, A. Dishlers, T. Kozlovska, V. Ose, P. Pushko, K. Tars, E. Grens, M. F. Bachmann, *Intervirology* **2016**, *59*, 74–110.

[66] A. Marini, Y. Zhou, Y. Li, I. J. Taylor, D. B. Leneghan, J. Jin, M. Zaric, D. Mekhaiel, C. A. Long, K. Miura, S. Biswas, *Front. Immunol.* **2019**, *10*, 2931.

[67] B. Nguyen, N. H. Tolia, *npj Vaccines* **2021**, *6*, 70.

[68] D. Pinto, Y.-J. Park, M. Beltramello, A. C. Walls, M. A. Tortorici, S. Bianchi, S. Jaconi, K. Culap, F. Zatta, A. De Marco, A. Peter, B. Guarino, R. Spreafico, E. Cameroni, J. B. Case, R. E. Chen, C. Havenar-Daughton, G. Snell, A. Telenti, H. W. Virgin, A. Lanzavecchia, M. S. Diamond, K. Fink, D. Veesler, D. Corti, *Nature* **2020**, *583*, 290–295.

[69] Y. Watanabe, J. D. Allen, D. Wrapp, J. S. McLellan, M. Crispin, *Science* **2020**, eabb9983.

[70] A. Antonopoulos, S. Broome, V. Sharov, C. Ziegenfuss, R. L. Easton, M. Panico, A. Dell, H. R. Morris, S. M. Haslam, *Glycobiology* **2020**, cwaa085.

[71] D. B. Leneghan, K. Miura, I. J. Taylor, Y. Li, J. Jin, K. D. Brune, M. F. Bachmann, M. Howarth, C. A. Long, S. Biswas, *Scientific Reports* **2017**, *7*, 1–14.

[72] M. L. Blackman, M. Royzen, J. M. Fox, *J. Am. Chem. Soc.* **2008**, *130*, 13518–13519.

[73] D. M. Klinman, D. Currie, I. Gursel, D. Verthelyi, *Immunol. Rev.* **2004**, *199*, 201–216.

[74] T. C. Williams, W. A. Burgers, *Lancet Respir Med* **2021**, *9*, 333–335.

[75] P. J. Shilling, K. Mirzadeh, A. J. Cumming, M. Widesheim, Z. Köck, D. O. Daley, *Commun Biol* **2020**, *3*, 214.

[76] D. Lauster, S. Klenk, K. Ludwig, S. Nojoumi, S. Behren, L. Adam, M. Stadtmüller, S. Saenger, S. Zimmler, K. Hönzke, L. Yao, U. Hoffmann, M. Bardua, A. Hamann, M. Witzenrath, L. E. Sander, T. Wolff, A. C. Hocke, S. Hippenstiel, S. De Carlo, J. Neudecker, K. Osterrieder, N. Budisa, R. R. Netz, C. Böttcher, S. Liese, A. Herrmann, C. P. R. Hackenberger, *Nat. Nanotechnol.* **2020**, *15*, 373–379.

[77] H. Jiang, W. Chen, J. Wang, R. Zhang, *Chin. Chem. Lett.* **2021**, DOI: 10.1016/j.cclet.2021.06.011.

[78] L. De Rosa, R. Di Stasi, A. Romanelli, L. D. D'Andrea, *Molecules* **2021**, *26*, 3521.

[79] A. M. Marmelstein, M. J. Lobba, C. S. Mogilevsky, J. C. Maza, D. D. Brauer, M. B. Francis, *J. Am. Chem. Soc.* **2020**, *142*, 5078–5086.

Entry for the Table of Contents

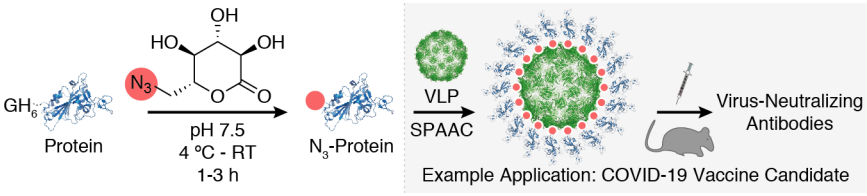

We report site-selective α-amino acylation of proteins with N-terminal Gly-HisTags using 6-azido-6-deoxy-glucono-1,5-lactone (6AGDL). To demonstrate the usefulness of this reaction, we multimerise the SARS-CoV-2 receptor-binding domain (RBD) protein antigen onto virus-like particles (VLPs) via strain-promoted alkyne-azide cycloaddition (SPAAC). The resulting COVID-19 vaccine candidate induces single-shot seroconversion, and virus-neutralizing antibodies in mice